JOURNAL OF Materials CHEMISTRY

Preparation of potassium beta aluminas by gel-to-crystallite conversion and their characterisation

V. Jayaraman,[a] G. Periaswami[a] and T. R. N. Kutty*[b]

[a]*Materials Chemistry Division, Indira Gandhi Centre for Atomic Research, Kalpakkam 603 102, India*

[b]*Materials Research Centre, Indian Institute of Science, Bangalore 560 012, India*

A novel method for the preparation of phase-pure K-β-alumina is reported by the gel-to-crystallite conversion method. Here, coarse gels of hydrated alumina $Al_2O_3 \cdot yH_2O$ ($80 < y < 120$) were reacted with ethanolic KOH, yielding crystalline K-inserted gibbsite or K-pseudoboehmite. Thermal decomposition of these precursors above 500 K yielded intermediate K-inserted boehmite. Above 1473 K, K-β-alumina was obtained *via* a modified K-χ-alumina intermediate. The stability range of K-β-alumina can be extended up to 1 : 17 ($K_2O : Al_2O_3$) by this method. The extended compositional range of stability of K-β-alumina is explained on the basis of the polysynthetic lamellae arising from the collapse of the layers adjacent to the K—O plane, as revealed by high resolution electron microscopy (HREM). The increased number of AlO_6 octahedra, in comparison to AlO_4 tetrahedra and the prevalence of distorted AlO_6 with two or more types of second nearest neighbour interaction is indicated from the solid state ^{27}Al MAS NMR studies. To obtain K-β''-alumina, Li^+ or Mg^{2+} had to be incorporated. The mechanistic aspects of the formation of K-β- and K-β''-alumina are described in detail.

Introduction

Beta-aluminas are a class of compounds with the general formula, $M_2O \cdot xAl_2O_3$ where M = Li, Na, K, Rb, Ag, NH_4^+ or H_3O^+. For sodium β-aluminas, where x is in the range of 5–7, the phase is β''-alumina, the high conducting phase. For x = 8–11, the phase is β-alumina, a phase exhibiting lower ionic conductivity.[1,2] We have reported the preparation of phase-pure (Na)-β''-alumina by a novel method of gel-to-crystallite (G–C) conversion.[3] In this method, the amorphous gel of hydrated alumina reacts with NaOH solution under wet chemical conditions to yield nanosized crystallites of sodium inserted gibbsite which on heat treatment at elevated temperatures converts to Na-β''-alumina through the intermediates, (Na)-boehmite and (Na)-γ-alumina, of spinel type structure. The hydrated alumina gel suspended in ethanolic NaOH under boiling conditions collapses owing to the abstraction of water from the gel cavities by ethanol and the simultaneous chemical influx of aliovalent Na^+ ions. As a result, the ion-pressure within the gel decreases and the amorphous gel network breaks down, giving rise to nanometer sized crystalline precursors. The preparative parameters *viz*., initial sodium hydroxide concentration, the nature of the organic solvent used and the gel characteristics play important roles in the stability of Na-β''-alumina as described, in detail in our earlier publication.[4]

Potassium-β-aluminas are considered to be the ideal precursor for the preparation of the proton conducting β-aluminas used in fuel cells,[5] owing to the similarity in ionic radius of H_3O^+ (r = 1.38 Å) with K^+ (r = 1.33 Å). Formation of K-β''-alumina is still disputed and is often considered impossible.[6] A recent report[7] gives a brief account of the preparation of K-β-aluminas by a solid state ceramic route using intermediate aluminas in the presence of magnesium oxide. Here, we report the synthesis of phase-pure K-β- and K-β''-aluminas using the gel-to-crystallite conversion method. The various intermediates in the conversion of the precursor crystallites to the final products are also presented.

Experimental

A hydrated gel of alumina, $Al_2O_3 \cdot yH_2O$ ($80 < y < 120$) was precipitated from aqueous solutions of $Al_2(SO_4)_3$ at pH *ca.* 8. The gel was washed thoroughly to remove foreign ion impurities and was suspended in ethanol containing potassium hydroxide. The reaction flask was fitted with a water-cooled reflux condenser and the air in the reactor was replaced by nitrogen. An alkali guard-tube was provided to prevent the ingress of CO_2 into the reactor chamber. The reaction mixture was agitated using a magnetic stirrer while maintaining boiling conditions for 6–8 h around 350 K. The solid product obtained was filtered and washed free of KOH with ethanol and oven-dried under a CO_2-free atmosphere. For the preparation of Li_2O stabilised K-β''-alumina, lithium hydroxide was added along with KOH in the G–C preparation. For MgO as the stabiliser, the isolated precursor from the G–C preparation was mixed with a measured amount of MgO and calcined. The amount of potassium retained in the crystalline precursors and the final product was analysed by atomic absorption spectroscopy (AAS) (Perkin Elmer, model 5000, USA). Thermogravimetry and differential thermal analyses were carried out using a TG/DTA model STA 1500 (Polymer Laboratory, UK). In order to identify the intermediates observed in the thermal analyses, isothermal mass loss studies were carried out. X-Ray powder diffraction patterns were obtained using a D-500 model (M/s Siemens, Germany) with Cu-Kα radiation. IR spectra were obtained using an FTIR spectrometer (Bomem, Canada). Solid state MAS NMR studies were carried out using a high resolution NMR spectrometer (Bruker, Germany) fitted with a magic angle spinning (MAS) device. The chemical shifts (δ) were recorded referenced to $Al(H_2O)_6Cl_3$ (1 M aqueous solution $\delta = 0$). High resolution transmission electron microscopy (HREM) was carried out with a JEOL-GEM 200CX transmission electron microscope operating at 200 kV and equipped with an ultra high resolution objective pole piece in the top-entry configuration. The crystallites were dispersed in butanol by sonication and deposited on a carbon grid. Thin crystals projecting through the holes in the carbon grid were selected and oriented with respect to the electron beam. Using the goniometer, the through-focus images with defocusing value up to 100 nm were recorded at a primary magnification of 3.7×10^5.

Results

Effect of initial concentration of KOH and the solvent ratio

The chemical compositions of the precursor phases and the products obtained upon calcination at 1673 K are given in

Table 1 Formation of precursors and products with various initial concentrations of KOH

K_2O/Al_2O_3[a]	K_2O/Al_2O_3[b]	$K_2O:Al_2O_3$[c]	precursor[d] phases	final phase[e]
0.152	0.055	1:17	K-PB	β
0.208	0.064	1:15	K-PB	β
0.575	0.076	1:13	K-PB+G*	β
0.690	0.083	1:12	K-PB+G*	β
0.773	0.099	1:10	K-PB+G*	β
1.128	0.126	1:8	K-G+PB*	β
1.450	0.134	1:7.5	K-G+PB*	β
1.689	0.137	1:7.3	K-G+PB*	β
2.000	0.138	1:7.3	K-G+PB*	β

[a]In reaction mixture. [b]In the obtained precursor. [c]In residue after heating to 1673 K. [d]K-PB = K-inserted pseudoboehmite; K-G = K-inserted gibbsite; *Minor phase. [e]After heating at 1673 K; β = K-β-alumina.

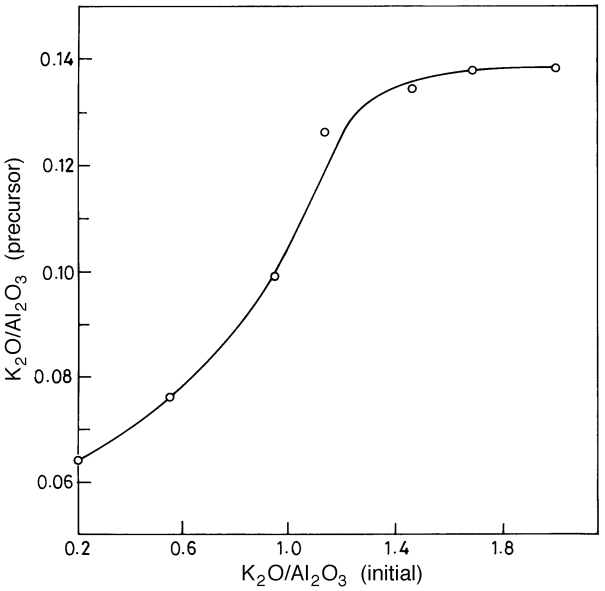

Fig. 1 K_2O/Al_2O_3 retained in the precursor as a function of the initial K_2O/Al_2O_3 used in the G–C preparation

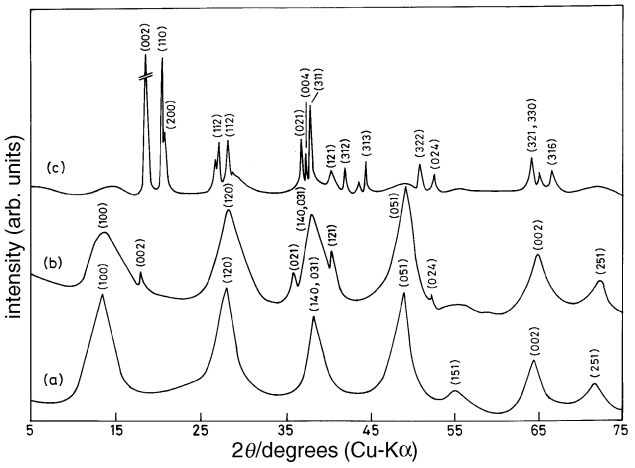

Fig. 2 XRD traces of the various precursor phases obtained for different K_2O/Al_2O_3 ratios: (a) 0.064, (b) 0.099 and (c) 0.126. Whereas phases in (a) and (b) are predominantly K-pseudoboehmites (c) is gibbsite according to diffraction studies.

Table 1. The K_2O contents in the crystalline precursor phases obtained from the G–C conversion increase with the K_2O/Al_2O_3 ratio in the reaction mixture (Fig. 1). K^+ inserted into the precursor crystallites having either gibbsite or pseudoboehmite structure increases proportionally up to the initial $K_2O/Al_2O_3 = 1.1$. The concentration of K^+ inserted in the precursor remains nearly constant above this ratio (Fig. 1). K-inserted pseudoboehmite crystallised as the major phase, with gibbsite as the minor phase when the initial K_2O/Al_2O_3 ratio was $\leqslant 0.8$. When K_2O/Al_2O_3 in the reaction mixture is between 1.1 and 2.0, K-gibbsite crystallised as the major phase. These samples on calcination above 1673 K yielded phase-pure K-β-alumina. XRD patterns of the precursors obtained are shown in Fig. 2.

The effect of varying ethanol/water (denoted solvent ratio) is studied with the initial K_2O/Al_2O_3 maintained around 0.7. The results are presented in Table 2. When the solvent ratio is around 2, maximum intake of K^+ was observed, with K_2O/Al_2O_3 *ca.* 0.08 in the recovered precursor crystallites. At solvent ratios <1.2, the intake of K^+ decreases steadily. The products therefrom yielded α-Al_2O_3 along with K-β-alumina on calcination at 1673 K, evidently due to the insufficient insertion of K^+ into the precursor crystallites.

Table 2 Effect of solvent ratio on the precursor and the final products[a]

EtOH/ water	$K_2O:Al_2O_3$ in precursor	precursor phases[b]	phases obtained after heating at 1673 K
1.72	1:12	K-PB+G*	β
1.29	1:17	K-PB+G*	β
0.86	1:22	K-PB	$\beta+\alpha$[c]

[a]Initial $K_2O/Al_2O_3 = 0.69$. [b]See footnote *d* of Table 1. [c]α = α-Alumina.

Thermal analyses and X-ray diffraction studies

Thermal analyses traces are presented in Fig. 3 for the samples prepared from reaction mixtures with various initial KOH concentrations in the G–C preparations. Similar DTA–TG patterns were obtained for the precursors with K_2O/Al_2O_3 ratios of 0.06 and 0.10, comparable with the thermal dehydroxylation curves of potassium-free pseudoboehmite [Al(O)OH·xH_2O]. A total mass loss of *ca.* 25% was observed up to 1273 K. According to TG curves, the mass loss takes place in two steps and the corresponding DTA peaks are at *ca.* 353 and 670 K. Evolved gas analyses showed water as the only product, indicating that the thermal decompositions are either dehydration or dehydroxylation. Thermal changes around 353 K can be attributed to the loss of adsorbed water amounting to 8%; the DTA peak around 670 K is due to dehydroxylation accompanied by a mass loss of 15%. For precursors having K_2O/Al_2O_3 of *ca.* 0.10, one more endothermic peak of low intensity was observed around 500 K. This could be attributed to the presence of K-gibbsite as the minor phase. As K_2O/Al_2O_3 increases, the endothermic peak observed at 670 K vanishes completely. A sharper endotherm is observed at 550 K along with a small peak around 500 K. The latter increases in intensity as K_2O/Al_2O_3 varies from 0.13 to 0.14 in the precursor (Fig. 3). A third shallow endothermic signal is observed at 775 K for the samples with high K_2O content, owing to further dehydroxylation of residual OH groups. No thermal changes are seen at high temperatures;

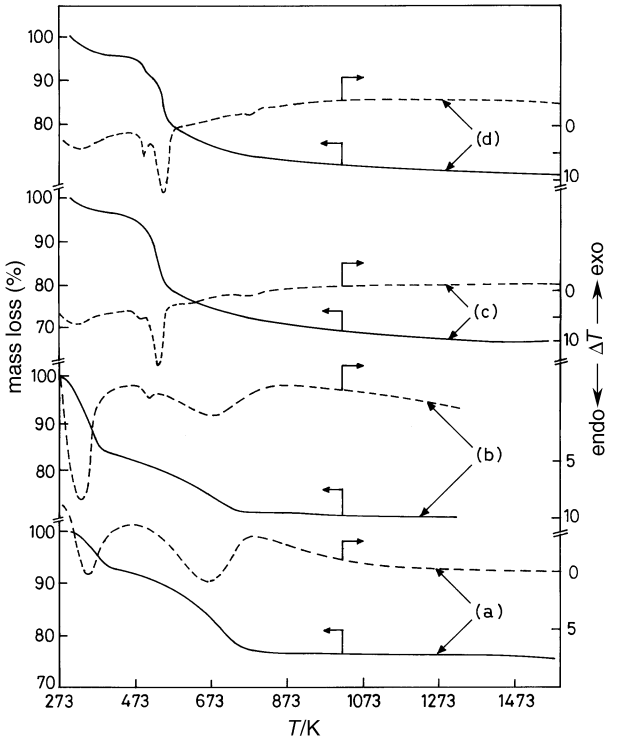

Fig. 3 TG–DTA traces of the precursors obtained with different K_2O/Al_2O_3 initial ratios: (a) 0.064, (b) 0.099, (c) 0.126 and (d) 0.137

particularly absent is the weak exothermic peak around 1473 K, typical of the transformation of intermediate aluminas to α-alumina. A similar observation was also reported for sodium inserted gibbsite.[3] The thermal event around 775 K is accompanied by a 5% mass loss amounting to a total of 30% for the K-gibbsite precursor.

In order to establish the compositions and identify the intermediates, isothermal heat treatments of the G–C conversion products were carried out around the temperatures at which changes were noticed in the DTA–TG curves, using the sample with $K_2O/Al_2O_3 = 0.13$. The samples were maintained at the desired temperatures until constant masses were obtained. The mass losses observed for the products are listed in Table 3 and the XRD patterns of the corresponding intermediates are shown in Fig. 4. The intermediate isolated at 523 K was K^+-inserted boehmite with dominant (020), (120), (140, 031), (051) and (002) reflections. The intermediates isolated at 723, 1073 and 1273 K were identical in composition. This was confirmed by isothermal annealing, wherein no mass loss was observed between 723 and 1273 K (Table 3). The XRD patterns of these two intermediates resemble that of χ-alumina with some modifications. The (100) reflection is absent and new reflections at $2\theta = 42$, 48 and 55° are observed. These modifications in the χ-alumina pattern can be attributed to the presence of larger K^+ ions in the cavities of the intermediate alumina network. On heating the samples to 1473 K, the K-

Table 3 Isothermal mass losses of the precursor having K_2O/Al_2O_3 0.13

		mass loss (%)	
T/K	duration/h	specific step	cumulative
378	72	0.67	0.67
523	54	22.07	22.74
723	21	5.36	28.10
1273	10	—	28.10
1673	5	5.10	33.20

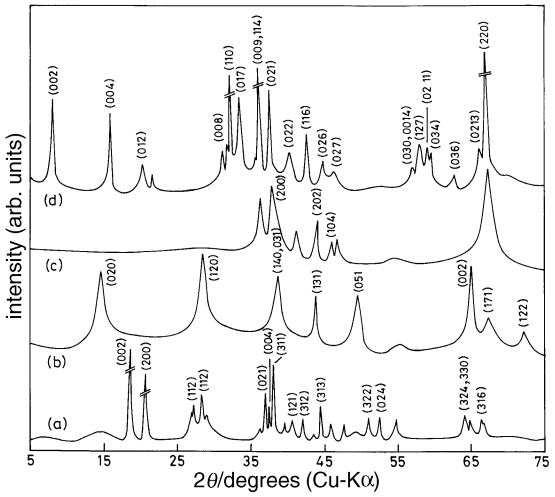

Fig. 4 XRD patterns of various intermediates obtained on heat treatment of the precursor having an initial K_2O/Al_2O_3 ratio of 0.13: (a) 378 K, (b) 523 K, (c) 1273 K and (d) 1473 K

β-alumina phase crystallizes with characteristic (002) and (004) reflections.

IR studies

IR spectra of the intermediates are presented in Fig. 5. The sample dried at 378 K showed a well resolved band in the O—H stretching frequency around 3630 cm^{-1} and can be assigned to terminal hydroxy groups. The absorption bands around 3523, 3455 and 3365 cm^{-1} arise from hydroxy groups that are involved in hydrogen bonding, as well as from bridged hydroxy groups. The presence of H_2O as water of hydration or surface adsorbed molecules is indicated by an IR absorption band around 1645 cm^{-1} corresponding to the bending mode of H_2O. Absorption bands in the 950–1140 cm^{-1} region correspond to the stretching modes of AlO_4 as well as Al—OH—Al groups. In the latter case, each of the hydroxy groups is bridged to neighbouring Al^{3+} ions. Absorption bands in the region 600–800 cm^{-1} arise from the stretching modes of AlO_6 as well as the librational mode of OH groups. Absorption bands below 600 cm^{-1} are attributed to the bending modes of vibrations of AlO_4 and AlO_6 groups. After heat treatment above 523 K, only the OH absorption around 3350 cm^{-1} persists. Disappearance of the higher frequency absorption indicates that the ionic as well as the terminal hydroxy groups have been eliminated during the thermal treatment. For

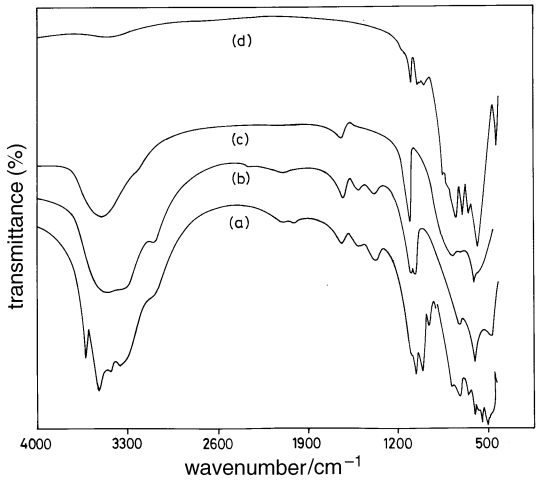

Fig. 5 IR spectra of the intermediates obtained on heat treatment of the precursor with an initial K_2O/Al_2O_3 ratio of 0.13: (a) 378 K, (b) 523 K, (c) 1073 K and (d) 1473 K

samples calcined above 1473 K, the only persisting absorption bands are due to AlO_4 and AlO_6 groups.

From these observations, the following reaction sequence for the formation of K-β-alumina can be postulated.

$$Al_2O_3 \cdot yH_2O\,(gel) + KOH \xrightarrow[350\,K,\,EtOH]{G\text{–}C\ conversion} K_2Al_{16}O(OH)_{48} \cdot 0.5H_2O \quad (K_2O:Al_2O_3 = 1:8)$$

$$\xrightarrow{378\,K} K_2Al_{16}O(OH)_{48} + 0.5H_2O \quad \text{K-gibbsite}$$

$$\xrightarrow{500\,K} K_2Al_{16}O_{17.5}(OH)_{15} + 16.5H_2O \quad \text{K-boehmite}$$

$$\xrightarrow{723\,K} K_2Al_{16}O_{21.5}(OH)_7 + 4H_2O \quad \text{modified } \chi\text{-alumina}$$

$$\xrightarrow{>1273\,K} K_2Al_{16}O_{25} + 3.5H_2O \quad \text{K-}\beta\text{-alumina}$$

The presence of potassium ions causes the conversion of initially formed product, K-inserted gibbsite from the G–C preparation into K-inserted boehmite under the present experimental conditions. On heating to 723 K, K-boehmite is converted to an intermediate modified χ-alumina and this phase persists up to 1273 K. High temperature treatment of this intermediate yields K-β-alumina.

Reaction of K_2CO_3 with K-β-alumina precursors

Fig. 6 shows the XRD trace obtained after calcining the G–C preparation product at 1673 K after wet mounting with K_2CO_3. Mounting of K_2CO_3 was done by a thorough mixing of the G–C product of $K_2O/Al_2O_3 = 0.137$ in acetone. The typical ratio of G–C product to K_2CO_3 was 1:3. After calcination, the products were washed with a water–ethanol mixture (10:90). The characteristic reflections of K-β''-alumina *viz.* (01,11) and (02,10) were observed. This pattern is compared with the as-prepared powder from G–C preparation annealed at 1673 K, wherein the characteristic β''-alumina reflections were not observed.

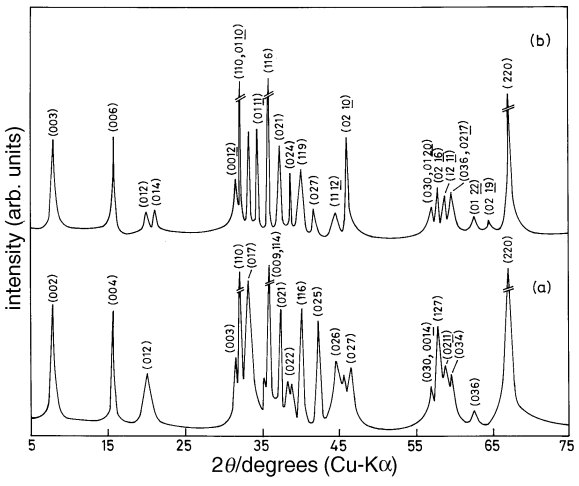

Fig. 6 XRD traces of the products calcined at 1673 K: (a) without K_2CO_3 and (b) after wet mounting with K_2CO_3

Effect of Li_2O and MgO

Table 4 shows the various precursor phases on addition of LiOH in the G–C conversions and the products obtained after calcination at 1673 K. When 4 mol% Li_2O was added ($Li_2O:K_2O:Al_2O_3 = 0.04:0.09:1$) in the G–C preparation, the precursor obtained was K-gibbsite. A similar preparation without Li_2O, yielded K-pseudoboehmite as the major precursor phase. Thus, the presence of Li_2O alters the characteristics of the resulting crystalline precursor. On increasing the Li_2O concentration to 7 mol% ($Li_2O:K_2O:Al_2O_3 = 0.08:0.09:1$), gibbsite is formed along with layered double hydroxide (LDH), $LiAl_2(OH)_7 \cdot 2H_2O$, as the minor phase. Li_2O-incorporated precursors yielded β''-alumina on calcination at 1673 K. Fig. 7 shows the XRD patterns of the various intermediates isolated on heat treatment at elevated temperatures. At 523 K, the intermediate isolated was K-boehmite which matches well with the intermediate obtained at this temperature for the lithium-free system. After heating at 723–1273 K, similar XRD traces are observed, indicating that the nature of the crystalline intermediate is the same in this temperature range. The XRD patterns of these samples match well with that of γ-alumina as against the χ-alumina phase obtained in Li-free preparations. The intermediate, K-γ-alumina, converts to β''-alumina after calcination at 1673 K. Further increase in Li_2O concentration to 9 mol% ($Li_2O:K_2O:Al_2O_3 = 0.11:0.09:1$), showed the presence of increased quantities of $LiAl_2(OH)_7 \cdot 2H_2O$. This mixed precursor on calcination yielded K-β''-alumina along with $LiAl_5O_8$ (lithium aluminium spinel). This is indicated by the diminished intensities of the (00*l*) reflections of β''-alumina

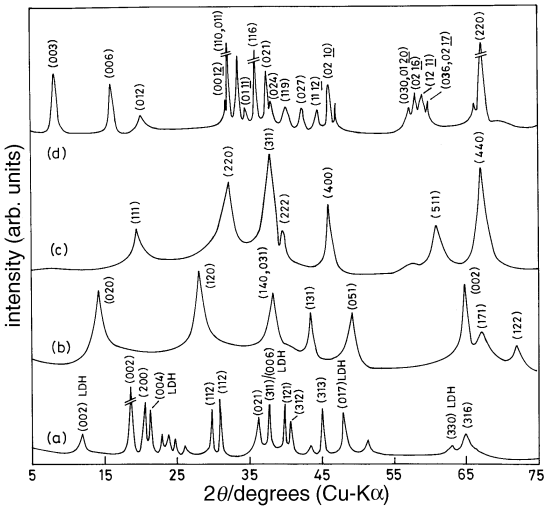

Fig. 7 XRD traces of the intermediates isolated on heat treatment of the precursor with $Li_2O:K_2O:Al_2O_3 = 0.08:0.09:1$ at (a) 378 K, (b) 523 K, (c) 1273 K and (d) 1673 K [LDH = layered double hydroxide, $LiAl_2(OH)_7 \cdot 2H_2O$]

Table 4 G–C conversion products partially stabilised with Li_2O

no. of mol of					
Li_2O	K_2O	Al_2O_3	Li_2O (mol%)	phases at 378 K[a]	phases after heating at 1673 K
—	0.09	1	—	K-PB	K-β-alumina
0.04	0.09	1	4.54	K-PB	K-β''-alumina
0.08	0.09	1	6.81	K-G + LDH*	K-β''-alumina
0.11	0.09	1	9.13	K-G + LDH	K-β''-alumina* + $LiAl_5O_8$

[a]See footnote *d* of Table 1; LDH = Layered double hydroxide, $LiAl_2(OH)_7 \cdot 2H_2O$.

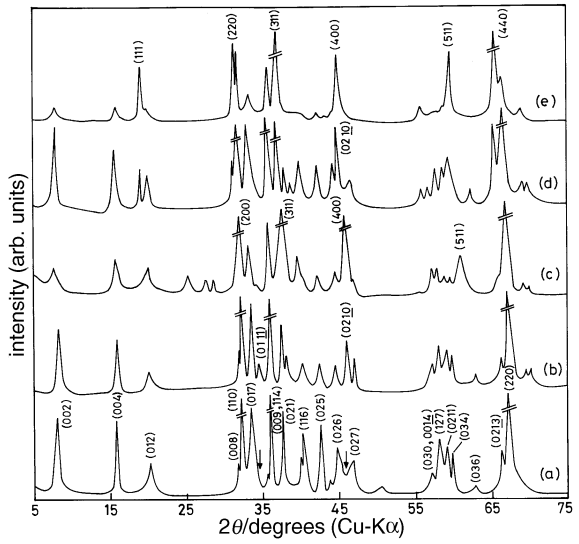

Fig. 8 XRD traces of the phases obtained on substitution with: (a) 0 mol%, (b) 4 mol% Li_2O, (c) 9 mol% Li_2O, (d) 3 mol% MgO and (e) 6 mol% MgO

phase and with the presence of (200), (311), (400) and (511) reflections of $LiAl_5O_8$ (Fig. 8).

Addition of 3 mol% MgO to the precursor, K-pseudo-boehmite, and subsequent calcination at 1673 K yielded K-β''-alumina as the only phase which was identified by the presence of (01,11) and (02,10) reflections (Fig. 8). On increasing the MgO concentration to 6 mol%, crystallisation of $MgAl_2O_4$ is observed, with diminished intensities of the (00l) reflections of K-β''-alumina. Formation of $MgAl_2O_4$ phase is evident from the (111), (220), (311), (400), (511) and (440) reflections (Fig. 8).

^{27}Al MAS NMR studies

Isotopic chemical shifts, in ^{27}Al NMR spectra are dependent upon the coordination number of AlO_x polyhedra ($x=4$, 5 or 6) and also the second nearest neighbour chemical environments. The MAS ^{27}Al NMR spectra of K-β-alumina samples with different K_2O/Al_2O_3 ratios are shown in Fig. 9, together with the spectra of the related phases for comparison. The spectrum [Fig. 9(b)] of the K-β alumina sample with $K_2O:Al_2O_3=1:17$ shows three maxima with δ values of -4.5, 14.1 and 65.1 with relative intensities of 1.7 : 1 : 1.1 (area integrated values). None of these are spinning side bands because they are not shifted with the spinning speed. The chemical shifts of AlO_6 occur around δ 0–10, AlO_5 around δ 30–40 and those of AlO_4 are around δ 55–80.[8] Furthermore, the chemical shifts in the region $\delta -10$ to $+10$ are attributed to the second nearest neighbour effect on the NMR of AlO_6 octahedra. Negative values of chemical shifts are reported for basic aluminium hydroxide by Müller *et al.*[8] Whereas the peak at δ 65 in Fig. 9(b) can be attributed to AlO_4 tetrahedra, those at $\delta -4.5$ and 14.1 are attributable to K-β-alumina because the MAS NMR of Na-β-alumina showed peaks [Fig. 9(c)] at δ 9 and 64 corresponding to AlO_6 and AlO_4, respectively. The peaks at δ 14 and 65 are reported for γ-alumina with spinel type structure wherein, the octahedral/tetrahedral intensity ratio deviates from the expected 2 : 1 value for the ideal spinel cation distribution. In contrast, the spectrum of α-Al_2O_3 with only AlO_6 in the lattice exhibits one peak at δ 5. Therefore, the peaks at $\delta -4.5$ and 14 can only be accounted for in terms of distorted AlO_6 with respect to the second nearest neighbour Al atoms, the first set having six-coordination whereas the second set is four coordinated. The combined intensity of the $\delta -4.5$ and 14 peaks to that of the δ 65 peak corresponds to 2.46 approaching that of γ-alumina (*ca.* 2.52) indicating a

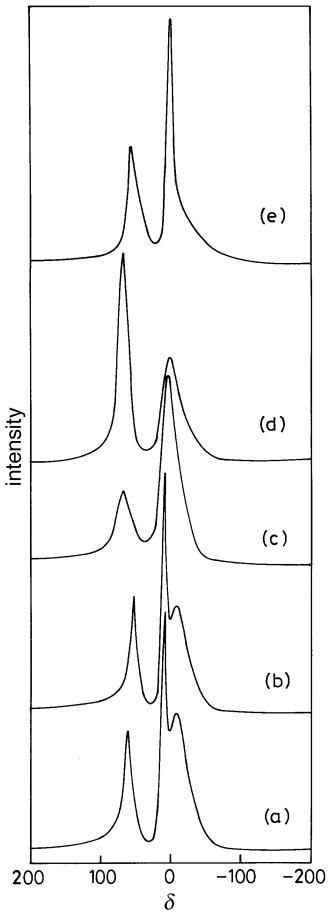

Fig. 9 Solid state ^{27}Al MAS NMR of (a) K-β-alumina sample with $K_2O:Al_2O_3=1:7$, (b) K-β-alumina sample with $K_2O:Al_2O_3=1:17$, (c) Na-β-alumina, (d) Ba-hexaaluminate and (e) K-β''-alumina with 5% Li_2O

higher number of octahedral Al than that of the 2 : 1 ratio of the spinel structure; in turn, the spinel blocks build up the β-alumina structure. The octahedral to tetrahedral ratio deviates from the expected value for Ba-hexaaluminate [Fig. 9(d)] wherein the dominance of tetrahedral aluminium is discernable from the intensity ratio. Structural similarity of the Ba-analogues to that of K-β-alumina is expected from the comparable radii of the Ba^{2+} and K^+ ions. It is clear that the deviation in spectral intensities has to be explained in terms of the cation ordering as well as prevalence of the extended defects as demonstrated by the HREM studies.

^{27}Al MAS NMR of K-β-alumina samples with higher K_2O contents [$K_2O:Al_2O_3=1:7$ Fig. 9(a)] show the same three peaks as described above. However, the chemical shifts increase with $K_2O:Al_2O_3$ ratio. The intensity of the peak at $\delta -4.5$ decreases to some extent. That the prevalence of the three peaks is related to the defects is also evident from the NMR of Li substituted K-β''-alumina samples. With 5% substitution of Li^+, the $\delta -4.5$ peak is negligible [Fig. 9(e)]. Its intensity decreases since Li occupies the spinel block at the octahedral sites and is charge compensated by the cation vacancies.

High resolution transmission electron microscopy

Selected area electron diffraction (SAED) and high resolution lattice imaging indicate that the K-β-alumina is more disordered at lower K_2O compositions. For samples with $K_2O:Al_2O_3=1:7$ (KAl_7O_{11}), the electron diffraction pattern obtained with the beam parallel to [10,10] shows equal intensity spots with a periodicity of *ca.* 2.25 nm along the c^* axis [Fig. 10(a)]. When $K_2O:Al_2O_3=1:17$ ($KAl_{17}O_{26}$), the c^* periodicity [Fig. 10(b)] corresponds to 1.12 nm with consider-

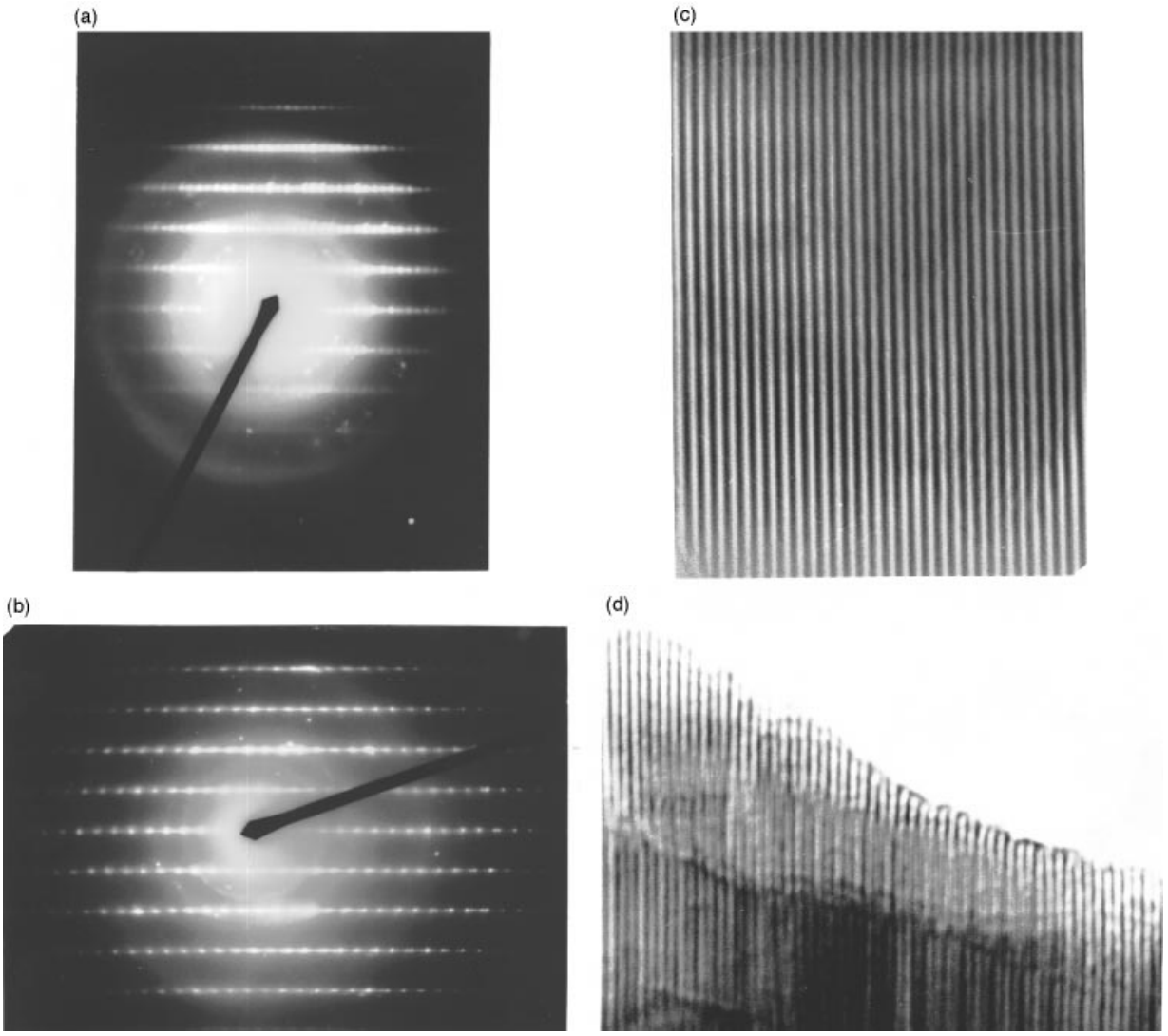

Fig. 10 Selected area electron diffraction (SAED) of (a) K-β-alumina (KAl_7O_{11}), (b) K-β-alumina ($KAl_{17}O_{26}$) and (c) and (d) high resolution lattice images of K-β-alumina (KAl_7O_{11})

able streaks along the same axis. The corresponding lattice images also show large differences. The dark fringes in Fig. 10(c) represent the image of the charge density of the cubic close packed spinel blocks whereas the white fringes in between correspond to the K^+-bearing ionic conduction layers.[9] The distance between black fringes in Fig. 10(c) is 1.13 nm which corresponds to $c/2$ for K-β-alumina. The uniform fringes in Fig. 10(c) indicate that there is hardly any difference in widths of the spinel blocks of the samples with $K_2O:Al_2O_3=1:7$. However in some regions of these samples the white bands merge with the dark fringes indicative of the blocking defects reported by Bovin[9] in Na-β-alumina [Fig. 10(d)]. For specimens with lower K_2O content, *e.g.* $K_2O:Al_2O_3=1:17$ ($KAl_{17}O_{26}$), polysynthetic twinning is evident from the high resolution micrographs wherein the widths of the twin lamellae are non-uniform and random. Some of the white fringes are broader than others and the wider white fringes appear at the boundaries of twin lamellae. Merging of the adjacent dark fringes into one fringe (marked by an arrow) (Fig. 11) and the presence of the blocking defects are indicative of the interrupted growth features with respect to the stacking of spinel blocks and the conducting layers. These features arise as a result of the deficiency of K^+ ions which, in turn, will affect the nature of the AlO_6 polyhedra.

The origin of such differences in lattice images can be explained in the following way: because of the deficiency of K^+ ions, oxygens in the interconnecting layers will be absent, which results in the collapse of the '*b*'-layer of the adjacent Al—O—Al bridges as shown schematically in Fig. 12. The two parts of the lattice on both sides of '*b*'-layer will move closer (*ca.* 0.22 nm) in the *c*-direction. As a result, the Al^{3+} ions of tetrahedral coordination will disappear and move to adjacent octahedral sites as shown in Fig. 12. The close packed three-layer slabs with face sharing octahedra will be more distorted than that of the corundum (α-Al_2O_3) structure. During this process, the individual parts will misalign leading to polysynthetic twin lamellae. It is well known that these close packed slabs cannot be deciphered from the micrograph because the resolution required would be <0.2 nm. It is evident from the schematic mechanism that the number of octahedral Al increases as also the next nearest neighbour coordination of AlO_6 will differ from that of ideal β-alumina. In the presence of stabilising substituents such as Li^+ or Mg^{2+} ions, the β-alumina structure will be free of extended defects by forming independent point defects (Al^{3+} vacancies) within the spinel blocks.

Discussion

Present studies, as also our earlier reports,[10,11] show that G–C conversion is a general technique for the preparation of nanosized multicomponent oxides such as aluminates, ferrites, zirconates, titanates, polytitanates, *etc.* In general, metal hydroxide gels are three-dimensional networks of polymeric

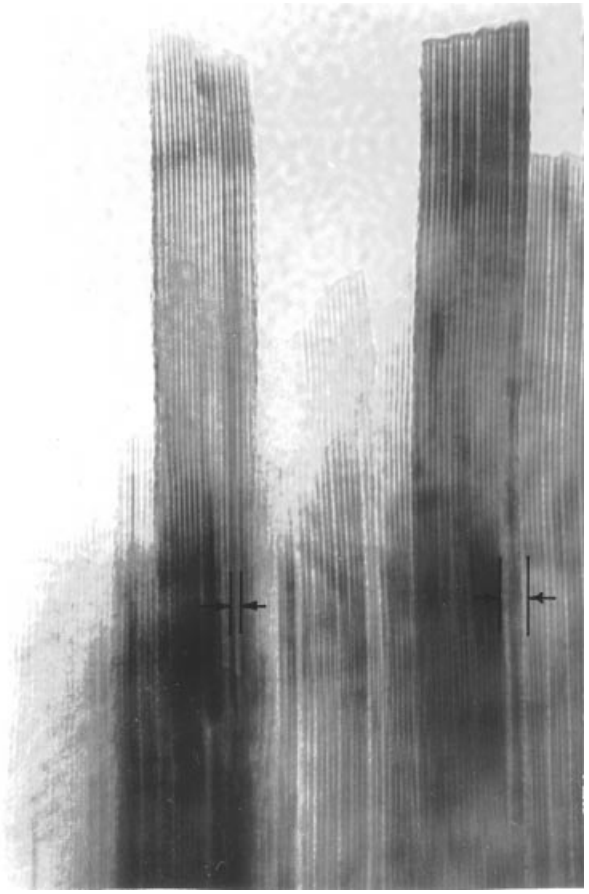

Fig. 11 High resolution electron microscopy (HREM) image showing the interrupted growth of K-β-alumina ($KAl_{17}O_{26}$)

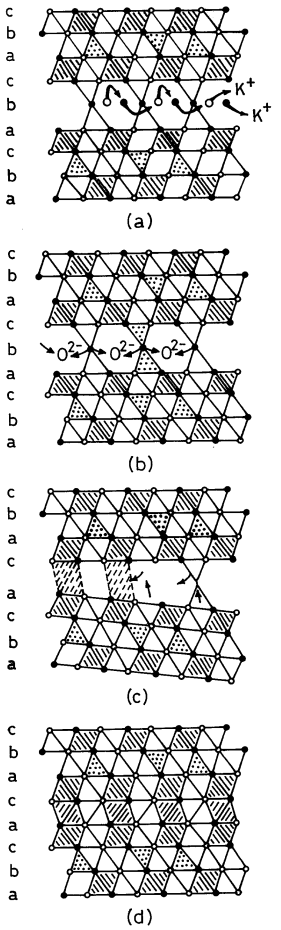

Fig. 12 Schematic diagram indicating the mechanism of formation of intergrowth lamellae in K-β-alumina ($KAl_{17}O_{26}$) (a) out diffusion of K^+ ions; (b) rearrangement of O^{2-} ions from the corners of the tetrahedra; (c) intermediate stage of formation of octahedra and (d) intergrowth lamellae with collapsed conduction plane leading to formation of three layer octahedral slabs

chains with entrapped solvent molecules (water). The gel, upon suspension in ethanol, undergoes solvent exchange between water from the gel matrix and ethanol from the surrounding medium. Because of the high affinity between ethanol and water, released water molecules cannot diffuse back into the gel network, which causes instability of the gel matrix. Simultaneous to the instability brought about by the solvent exchange is the rapid inflow of the aliovalent ions (K^+ in this case) into the gel cavities which upsets the charge balance. Hence, the system has to rearrange itself to maintain electrical neutrality (due to the inflow of K^+ ions). Since there is a continuous influx of ions, the interactive stability between the gel network and the solvent breaks down leading to fine nanocrystallites as products.

When compared to the preparation of Na-β'' or β-alumina using G–C conversion methods,[3] the initial ratio of $Na_2O/Al_2O_3 = 0.4$ yields Na-gibbsite precursor with $Na_2O/Al_2O_3 = 0.182$. The precursor is nearly saturated with Na^+ thereafter, whereas, for K-β-alumina preparations, saturation begins with a high initial ratio of $K_2O/Al_2O_3 \approx 1.4$ and the maximum amount of K^+ inserted corresponds to K_2O/Al_2O_3 *ca.* 1:7. It is known that gibbsite and boehmite have open structures containing channels along the [001] direction,[12] in which aliovalent ions (*e.g.*, sodium or potassium) can be accommodated. The difference in behaviour between sodium and potassium ions can be attributed to the larger size of K^+ ($r = 1.33$ Å) and thereby the insertion of K^+ ions into the gel network becomes more difficult. Furthermore, the affinity of ethanol towards KOH is higher than that towards NaOH.[13] Thus, larger concentrations of KOH are required to attain the saturation value. These arguments are confirmed by the formation of the K-pseudoboehmite phase at lower concentrations of KOH and K-gibbsite at higher concentrations (Table 1). The important point is the stability of K-β-alumina phase in the composition range of 1:7–1:17 (Table 2). The stability of the β-phase even at lower concentrations of K_2O is achievable because of the special route currently adopted, *i.e.* the G–C conversion method. This is a unique observation from this study.

During the preparation of Na-β''-alumina, the Na-gibbsite precursor gave rise to Na-boehmite on heating at 523 K. The intermediate, Na-inserted boehmite, was converted to Na-γ-alumina with a defect spinel structure at 723 K and to Na-β''-alumina on calcination at 1273 K. This observation indicates that an intermediate with cubic close packing of oxygen ions is a necessary step for the formation of β''-alumina[3,14] as the conversion of Na-γ-alumina to the Na-β''-alumina phase is a continuous solid state process with minimal rearrangement of close packed layers. For the potassium analogue, when a stabiliser such as Li_2O is incorporated, the precursor, K-gibbsite, on heating at 523 K, gave rise to K-boehmite. It is known that under certain reaction conditions such as high pressure, fast heating rates and large particle size, gibbsite can be converted to boehmite.[15] The particles of G–C conversion products are sub-micrometer in size; therefore, the presence of potassium ions causes the conversion of gibbsite to boehmite. The K-boehmite phase is converted to K-γ-alumina on heating to 723 K and persists up to 1273 K and converts to K-β''-alumina phase at higher temperatures. This observation confirms the necessity of the intermediate (K,Na)-γ-alumina phase in crystallising the β''-alumina phase for both the Na and K systems. In the absence of a stabiliser, on heating the K-boehmite intermediate to 723 K, the K-χ-alumina phase forms.

K-χ-alumina is stable up to 1273 K and converts into K-β-alumina upon further heating. In the absence of any stabiliser, reaction with an excess of K_2CO_3 is necessary for the formation of K-β''-alumina at 1673 K. The major reason for the difference in behaviour, when comparing with sodium analogues, is the lower degree of K^+ insertion in the precursors. The maximum insertion of K^+ corresponds to a composition of $K_2O:Al_2O_3$ of *ca.* 1:7 which is in the (borderline) limiting concentration range for the K-β''-alumina phase. Because of the lower concentration of K^+ ions, K-boehmite gives rise to poorly crystalline K-χ-alumina which, in turn, leads to the formation of K-β-alumina on calcination.

Conclusions

The gel-to-crystallite conversion method can be easily adapted for the preparation of a range of K-β-aluminas with K_2O to Al_2O_3 ratios varying from 1:7 to 1:17. Preparation of K-β-alumina with K_2O to Al_2O_3 ratio of 1:17 is only achievable by this technique. Formation of potassium deficient β-alumina is attributed to the existence of stacking defects of the spinel blocks. K-β''-alumina is obtained by incorporating lithium in the G–C preparative step followed by calcination or by mixing of the precursor obtained from the G–C method with magnesium oxide with subsequent calcination. Stabiliser free K-β''-alumina is obtained by calcining the precursor with excess potassium carbonate.

References

1 J. L. Sudworth and A. R. Tilley, *The Sodium Sulphur Battery*, Chapman and Hall, London, 1985.
2 J. T. Kummer, *Prog. Inorg. Chem.*, 1972, **7**, 141.
3 T. R. N. Kutty, V. Jayaraman and G. Periaswami, *Mater. Res. Bull.*, 1996, **31**, 1159.
4 V. Jayaraman, G. Periaswami and T. R. N. Kutty, *Mater. Chem. Phys.*, in press.
5 A. Tan and P. S. Nicholson, *Solid State Ionics*, 1988, **26**, 217.
6 G. M. Crosbie and G. J. Tennenhouse, *J. Am. Ceram. Soc.*, 1982, **65**, 187.
7 A. P. de Kroon, G. W. Schafer and F. Aldinger, *Chem. Mater.*, 1995, **7**, 878.
8 D. Müller, W. Gessner, H.-J. Behrens and G. Scheler, *Chem. Phys. Lett.*, 1981, **79**, 59.
9 J. Bovin, *Acta. Crystallogr., Sect. A*, 1979, **35**, 572.
10 P. Padmini and T. R. N. Kutty, *J. Mater. Chem.*, 1994, **4**, 1875.
11 T. R. N. Kutty and M. Nayak, *Mater. Res. Bull.*, 1995, **30**, 325.
12 K. Wefers, in *Alumina Chemicals: Science and Technology Handbook*, ed. L. D. Hart, American Ceramics Society, OH, 1990, pp. 13–22.
13 *Solubilities of Inorganic and Organic Compounds*, ed. H. Stephen and T. Stephen, Pergamon Press, Oxford, 1979, vol. 1 and 2.
14 A. van Zyl, M. M. Thackeray, G. K. Duncan, A. K. Kingon and R. O. Heckroadt, *Mater. Res. Bull.*, 1993, **28**, 145.
15 H. C. Stumpf, A. S. Russel, J. W. Newsome and C. M. Tucker, *Ind. Eng. Chem.*, 1950, **42**, 1398.

Paper 7/08079D; *Received* 10*th November*, 1997